On The Diffusion of Sticky Particles in 1-D

Joshua DM Hellier[*] and Graeme J Ackland[†]

SUPA, School of Physics and Astronomy, University of Edinburgh,
Mayfield Road, Edinburgh EH9 3JZ, United Kingdom
(Dated: June 29, 2017)

This is where I would write the abstract. This is probably best left until the end, as then I'll know what I'm actually summarising.

FIG. 1. Filled circles indicate particles, empty circles indicate empty sites (vacancies). Particles randomly move into adjacent vacancies with rate 1 (having rescaled time for notational convenience), unless there is a particle behind the position they're moving from, in which case they move with rate $\lambda = 1 - \zeta$.
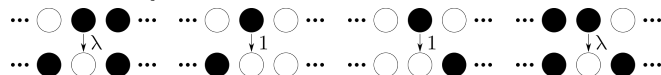
I. INTRODUCTION

Lattice gases are a ubiquitous tool for modelling complex systems from biology to traffic[1, 2]. One example is the oxidation process, as occurs in the growth of an oxide layer on a metallic surface. Almost all uncoated metallic objects [Al, Ti, Ca, Zr, Sn] are protected by such a thin, self-assembling layer, driven by the oxidation potential but arrested by the slow kinetics of transporting material through the oxide layer [3–6].

Analytically solvable cases involve non-interacting or excluding particles [7, 8]. But in any real system of interest the moving objects interact. Many models tackle the situation where the diffusing object interact with the substrate, but despite the clear application-relevance there is surprisingly little work considering interactions between the moving particles. One reason for this is that the interactions introduce nonlinearities in analytical models, which makes them challenging to solve. This is unfortunate, because it is precisely these nonlinearities which introduce interesting behaviours - discontinuities at the oxide-metal interface, diffusion instability, to name just a few. In this paper we will introduce (or perhaps more properly, revive) a simple 1-dimensional model, specified in Figure 1, which contains such an interaction, and we will explore the impact this has, particularly on behaviour in the large-scale limit. One might compare and contrast this approach (making a simple microscopic model and trying to learn about large-scale interface growth from it) with approaches such as the KPZ equation [9, 10].

---

[*] J.D.M.Hellier@sms.ed.ac.uk
[†] G.J.Ackland@ed.ac.uk

A. Model Definition

Our model, which we will refer to as the "Sticky Particle Model" or SPM, is essentially the same as the symmetric exclusion process [11], the difference being that adjacent particles separate with rate $\lambda = 1 - \zeta$ instead of their normal hopping rate, 1. It is in fact a rephrasing of the KLS model [12, 13] in 1-dimension without an applied field, which is itself similar to the dynamics used to analyse the Ising model by Kawasaki [14]. It seems that this symmetric model has not been researched much, at least in terms of its dynamics, because the model with the applied field is so interesting; however, it seems that the simple symmetric model is also capable of doing interesting things under an applied concentration gradient.

We have chosen to specify things primarily in terms of ζ instead of λ because it makes many of the analytic results much neater, whilst intuitively representing "stickiness", as particles tend to clump when $\zeta > 0$ and separate when $\zeta < 0$. It is worth noting that the rates specified in Figure 1 obey detailed balance, with an energy proportional to the number of particle-particle adjacencies in the system. One can show that there exists an isomorphism between this model and the Misanthrope Process [15]. This doesn't help us to solve the model in the kinds of steady flow cases we are mainly interested in due to difficulties with the boundary conditions, but it does allow us to show that this model does **not** exhibit explosive condensation [16].

II. MODEL PHENOMENOLOGY

The model described in Figure 1 is very simple, but numerical simulation shows that it is capable of a wide range of behaviours, such as those shown in Figure 3. We will discuss these numerical results in more detail in Section III, but first let us try to predict the model behaviour using analytic means.

A. Mean-Field Theory Derivation

Let the spacing between lattice sites be a, τ_0 be the non-sticky hopping timescale and the time-averaged (or ensemble-averaged, assuming ergodicity) occupation probability of the ith lattice site be ρ_i. One may show

that, in the mean-field approximation regime,

$$\tau_0 \frac{\partial \rho_i}{\partial t} = (1 - \rho_i) \left[(1 - \zeta \rho_{i-2}) \rho_{i-1} + (1 - \zeta \rho_{i+2}) \rho_{i+1} \right]$$
$$- \rho_i \left[2\zeta \rho_{i-1} \rho_{i+1} - (3 - \zeta)(\rho_{i-1} + \rho_{i+1}) + 2 \right],$$

.

Switching to the continuum limit by taking $a \to 0$, and neglecting $\mathcal{O}(a^4)$ terms, we may reexpress this as a conserved flow J as follows:

$$\frac{\partial \rho}{\partial t} = -\frac{\partial J}{\partial x},$$
$$J = -\frac{a^2}{\tau_0} A(\rho) \frac{\partial \rho}{\partial x},$$
$$A = 1 - \zeta \rho (4 - 3\rho).$$

Thus, the MFT says that the particles should diffuse with a diffusion coefficient which depends upon the local density.

B. Continuum MFT Predictions

First let us consider some limits. As $\zeta \to 0$ (in other words, as the model becomes a simple exclusion model), $A \to 1$, which makes sense. Likewise, in the dilute limit $\rho \to 0$, $A \to 1$, reflecting the fact that it becomes a dilute lattice gas and therefore the interactions between particles become irrelevant as they never meet. Conversely, in the full limit $\rho \to 1$, $A \to 1 - \zeta$; this makes sense because we now have a dilute gas of vacancies, which hop with rate $\lambda = 1 - \zeta$. One may observe that the continuum limit MFT has a symmetry under $\rho \mapsto \frac{4}{3} - \rho$; thus, the dynamics should be symmetric under a density profile reflection around $\rho = \frac{2}{3}$. This is where A always attains its extremal value, $1 - \frac{4}{3}\zeta$, hence for $\zeta > 3/4$ the diffusion coefficient becomes negative in regions with $\frac{2}{3} - \frac{\sqrt{\zeta(4\zeta-3)}}{3\zeta} < \rho < \frac{2}{3} + \frac{\sqrt{\zeta(4\zeta-3)}}{3\zeta}$. Finally, it is possible to show that solutions to the continuum MFT containing domains with a negative diffusion coefficient are linearly unstable; thus, if we try to have a flow containing ρ for which $A(\rho) < 0$, the density of the medium should gravitate towards a density for which $A(\rho) \sim 0$, so instead of observing "backwards diffusion" we would see an extremely slow flow or no flow at all.

C. MFT Solutions

1. Steady-State Flow Through a Block

It is possible to solve the continuum MFT in a steady state on a finite domain, say $x \in (0, L)$. The continuity equation implies that $J(x) = J_0$, and by integrating both

sides of our current equation with respect to x we find that

$$J_0(x - x_0) = -\frac{a^2}{\tau_0} \rho \left[1 + \zeta \rho (\rho - 2) \right], \qquad (1)$$

a cubic equation which can be solved to give $\rho(x)$. If we impose Dirichlet boundary conditions on this system, say $\rho(0) = \rho_0$ and $\rho(L) = \rho_L$, we find that

$$J = \frac{a^2}{L\tau_0} \left[\rho_0 - \rho_L + \zeta \left(\rho_0 \left[\rho_0^2 - 2 \right] - \rho_L \left[\rho_L^2 - 2 \right] \right) \right]. \quad (2)$$

We may consider applying small concentration gradients across a block by setting $\rho_0 = \rho_M + \frac{1}{2}\delta\rho$ and $\rho_L = \rho_M - \frac{1}{2}\delta\rho$. Doing so, we find that the effective diffusion coefficient of the block $D = \frac{\partial J}{\partial \delta\rho}\big|_{\delta\rho=0}$ obeys

$$\frac{\partial J}{\partial \delta\rho}\bigg|_{\delta\rho=0} = \frac{a^2}{L\tau_0} \left[1 - \zeta \rho_M (4 - 3\rho_M) \right], \qquad (3)$$

a result we will make use of when we come to analyse our numerics in Section III.

2. Constant Speed Solution

According to Ivanova [17], we can have travelling solutions to our time-dependent MFT PDE. Introducing the variable $\omega = x - vt$, with $v \in \mathbb{R}$, our PDE solution $\rho(x, t) = \phi(\omega)$ obeys

$$v\phi' = -\frac{a^2}{\tau_0} \left[1 - \zeta\phi (4 - 3\phi) \right]' \qquad (4)$$

with general solution found by solving

$$\omega = \frac{a^2}{\tau_0 v} \left[\frac{1}{2}\zeta\phi (8 - 6\mu - 3\phi) - (1 - \zeta [4 - 3\mu] \mu) \log (\phi - \mu) \right].$$
$$(5)$$

Requiring that $\phi \to 1$ as $\omega \to 0$ and $\phi \to 0$ as $\omega \to \infty$, this reduces to

$$\omega = \frac{a^2}{\tau_0 v} \left[\frac{1}{2}\zeta\phi (8 - 3\phi) - \log (\phi) - \frac{5\zeta}{2} \right], \qquad (6)$$

so at the leading edge of the wave, $\omega \to \infty$, $\phi \sim e^{-\frac{v\omega}{a^2}}$. At $\omega \to 0$ with $\phi \to 1$, which would physically represent the interface between the particle-saturated region and the non-saturated region, $\phi \sim 1 - \frac{v\omega}{a^2\lambda}$. Note that the value of v is not restricted by these equations, and a linear stability analysis of the leading edge does not imply speed selection like in the case of the Fisher wave[18], so it seems like the speed of travelling wavefronts would be determined by the initial conditions; of course, we should expect the MFT to misbehave close to the interface, so the actual system would probably have some interface-based mechanism for choosing its wave-speed.

3. Self-Similar Diffusive Solution

Again using Ivanova's work [17], we see that there should be a self-similar solution in the same vein as the erf $xt^{-\frac{1}{2}}$ solution for the normal diffusion equation. If we now let $\omega = xt^{-\frac{1}{2}}$, and again have $\rho(x,t) = \phi(\omega)$, this time ϕ must obey

$$\omega\phi' = -2\frac{a^2}{\tau_0}\left(\left[1 - \zeta\phi(4 - 3\phi)\right]\phi'\right)'. \tag{7}$$

Of course, for $\zeta \neq 0$ this is nonlinear in ϕ', and therefore extremely unlikely to have closed-form solutions; however, this is something which we would like to properly explore in the future.

III. NUMERICAL RESULTS

We now have some MFT predictions about the SPM, and a few ideas about when those predictions might be invalid. Thus, it is prudent for us to test them out numerically. There are a few different methods which could have been used, but we chose to calculate using the excellent `KMCLib`[19] package, which implements the Kinetic Monte Carlo algorithm (essentially the same as the Gillespie algorithm) on lattice systems. `KMCLib` has the advantage that it is python-wrapped `C++`, and thus quite easy to use whilst at the same time being quite computationally efficient; thus it was fairly easy for us to carry out large numbers of differently-parametrised serial `KMCLib` jobs on the `Eddie3` computing cluster here at Edinburgh. The codes used are kept here [20].

A. Flow in a Block

As we have MFT predictions about flow in a block, we can try to simulate that situation using KMC. In the bulk, the transition rates are simply those described in Figure 1. At the boundaries, referred to as the "top" and "bottom" of the block, there are 2 layers of lattice sites what switch between being full and empty with rates such that the time-averaged occupation can be specified to match the desired boundary conditions; there are then chances for particles to spawn and despawn with rates depending upon the occupation of these boundary layers. In the end, the intention is that these boundaries should reproduce the effect of having particle reservoirs attached to the ends, which is something we can check for sanity in the output by inspecting the time-averaged occupations of sites near the boundary.

In our calculations, we set the top and bottom densities to be $\rho_T = \rho_M - \frac{1}{2}\delta\rho$ and $\rho_B = \rho_M + \frac{1}{2}\delta\rho$ respectively, as well as specifying the value of λ and the number of sites in the lattice. During the calculation, we perform a specified number of Gillespie steps, and count the number of particles entering at the top e_T, leaving at the top l_T, entering at the bottom e_B, leaving at the bottom l_B, as well as the Gillespie time interval T that elapses during those steps; we then have an estimate of the overall flow rate J via

$$J = \frac{e_B - e_T + l_T - l_B}{2T}. \tag{8}$$

We can also count the total number of particles in the system in order to measure the average particle density, although we need to make sure that it is correctly time-averaged. If we keep $\delta\rho$ relatively small, J varies approximately linearly with $\delta\rho$; thus if we calculate J for a series of small $\delta\rho$, we can perform linear regression to find $D = \frac{\partial J}{\partial\delta\rho}\big|_{\delta\rho=0}$, the effective diffusion coefficient. Computing this for different (ρ_M, λ) combinations gives us numerical data which can be compared with the MFT result in Equation 3. To produce the results in Figure 2, for each $(\rho_T, \rho_B, \lambda)$ combination we created the initial state by randomly inserting particles into an empty 124-length lattice, so that the density was ρ_M. We then ran the simulation for 1.6×10^8 steps, to wash away any spurious initial-data effects and allow the system to reach a steady state flow. We then ran for 8×10^7 steps whilst measuring flow rate and density, then allowed the system to run for 1.6×10^7 steps without taking measurements in an effort to suppress temporal autocorrelation effects. This alternating process was repeated 10 times, yielding 10 measurements of flow rate and density, from which estimates of these quantities and their standard errors could be obtained. The whole setup was repeated with a 60-length system, in order to check for edge effects; however, the results were not significantly different, so those would not seem to be a problem.

We can of course obtain estimates of the confidence interval for our linear regression coefficient, and thus generate a standard error for D; likewise we can obtain goodness of fit estimates for the regression. They are not included here due to space constraints, but they are in the additional materials.

B. Flow Structure

It is possible to produce diagrams which show the changes in short-time-averaged local density as a function of space and time. I have made such diagrams for a selection of (ρ_M, λ) pairs, so that the reader can get an impression of what these flows actually look like; they are shown in Figure 3.

IV. DISCUSSION

A. Diffusion Coefficient

Putting the MFT prediction and the actual numerical results together as we have done in Figure 2, we can compare and contrast. The MFT seems to be a good

predictor of the true behaviour of the diffusion coefficient, including the strange symmetry about $\rho_M = \frac{2}{3}$ we pointed out in Section II B, so long as we avoid the region where the MFT predicts $D < 0.4$. The incorrectness of the MFT prediction suggests that some kind of nontrivial correlations have built up in this region, which makes sense as the coupling between particles has become stronger, whilst the density is middling, allowing that coupling to mean something. It is also worth noting that the discrepancy between intended density and actual density starts to become non-negligible here, which we can infer from how the originally rectangular grid of grey dots (indicating (ρ_M, λ) points where we obtained the data) has been deformed, to the extent that there is a big cluster of them in the observed minimum of the diffusion coefficient. Some of these anomalous densities are greater than the density of the denser reservoir to which the system is coupled; thus, the reservoirs involved are in some sense "unphysical" as the data suggests that they would immediately attempt to switch to a higher density, which given a constant volume constraint would imply a phase separation occurs; thus the numerical results aren't fitting so well into the paradigm we were using to analyse them (flow between reservoirs with slightly different densities), so it's little wonder the MFT is having trouble keeping up. Of course, we do not see the negative diffusion coefficient that naive application of MFT would suggest, because it would cause instability; instead, the diffusion coefficient just becomes very small, as the system becomes unresponsive to concentration gradients.

B. Flow Structure

Looking at Figure 3, we can make some observations. When λ is extremely low, the medium consists of solid blocks surrounded by empty spaces containing a dilute gas of particles; as we alter the overall density, all that changes is the thicknesses of these blocks. The case $\lambda = 1$ is just excluded Brownian motion, and is included here for comparison. The most interesting images are those for the intermediate (ρ_M, λ); here we see a "lumpy" or "foamy" structure, in which small blocks of particles are being constantly created and destroyed whilst a rather minimal flow occurs across the system. We do not think that there is any hard phase transition as we vary (ρ_M, λ); rather, it seems that this "foamy" behaviour is part of a continuous range of phenomena between the extremes, containing medium-range correlations between particles. However, numerically computing equal-time correlation functions to the accuracy required to draw conclusions about these correlations has proven to be extremely difficult, so we cannot speak in quantitative terms about them.

C. Conclusions

To conclude, the continuum MFT is a surprisingly good predictor of the bulk flow behaviour of the SPM, provided we avoid the region where it breaks down. That, combined with interpolations of our data about the flows during breakdown, could form the basis of a large-scale approximation of the flow, which could be used to make a PDE model of, say, interface growth on metal surfaces. Further study is required, of course; in particular it would be interesting to generalise this model to multiple species inhabiting coupled lattices, as this could inform us about the oxidation of alloys, such as niobium-enriched titanium.

[1] V. Belitsky and G. M. Schtz, Journal of Statistical Mechanics: Theory and Experiment **2011**, P07007 (2011).

[2] M. Mobilia, I. T. Georgiev, and U. C. Täuber, Journal of Statistical Physics **128**, 447 (2007).

[3] B. Tegner, L. Zhu, C. Siemers, K. Saksl, and G. Ackland, Journal of Alloys and Compounds **643**, 100 (2015).

[4] L. Zhu, Q.-M. Hu, R. Yang, and G. J. Ackland, The Journal of Physical Chemistry C **116**, 24201 (2012).

[5] B. E. Deal and A. Grove, Journal of Applied Physics **36**, 3770 (1965).

[6] N. Cabrera and N. Mott, Reports on progress in physics **12**, 163 (1949).

[7] A. J. Ladd, M. E. Colvin, and D. Frenkel, Physical review letters **60**, 975 (1988).

[8] T. M. Liggett, *Interacting particle systems* (Springer-Verlag, Berlin, 1985).

[9] M. Kardar, G. Parisi, and Y.-C. Zhang, Phys. Rev. Lett. **56**, 889 (1986).

[10] J. Krug and H. Spohn, Phys. Rev. A **38**, 4271 (1988).

[11] K. Sugden and M. Evans, Journal of Statistical Mechanics: Theory and Experiment **2007**, P11013 (2007).

[12] S. Katz, J. L. Lebowitz, and H. Spohn, Journal of Statistical Physics **34**, 497 (1984).

[13] R. K. P. Zia, Journal of Statistical Physics **138**, 20 (2010).

[14] K. Kawasaki, Phys. Rev. **145**, 224 (1966).

[15] M. R. Evans and B. Waclaw, Journal of Physics A: Mathematical and Theoretical **47**, 095001 (2014).

[16] B. Waclaw and M. R. Evans, Physical review letters **108**, 070601 (2012).

[17] N. M. Ivanova, arXiv preprint arXiv:0710.4000 (2007).

[18] J. A. Sherratt, Dynamics and Stability of Systems **13**, 167 (1998).

[19] M. Leetmaa and N. V. Skorodumova, Computer Physics Communications **185**, 2340 (2014).

[20] J. Hellier, "Codes for Sticky Particles in 1D," (2017).

FIG. 2. The contour plot on the left shows the MFT prediction of the diffusion coefficient $D = \frac{\partial J}{\partial \delta \rho}\big|_{\delta\rho=0}$ as a function of local density ρ_M and λ; we are only plotting where $0 \leq D \leq 1.2$, other regions are shown in white, including the region in which $D < 0$, which would cause instabilities and so prevent a flow from actually occurring. On the right is our numerical calculation of $D(\rho_M, \lambda)$, with exactly the same plotting ranges. The dots indicate which points in (ρ_M, λ) we calculated D around, to give an impression of how the interpolation in the contour plot was done.
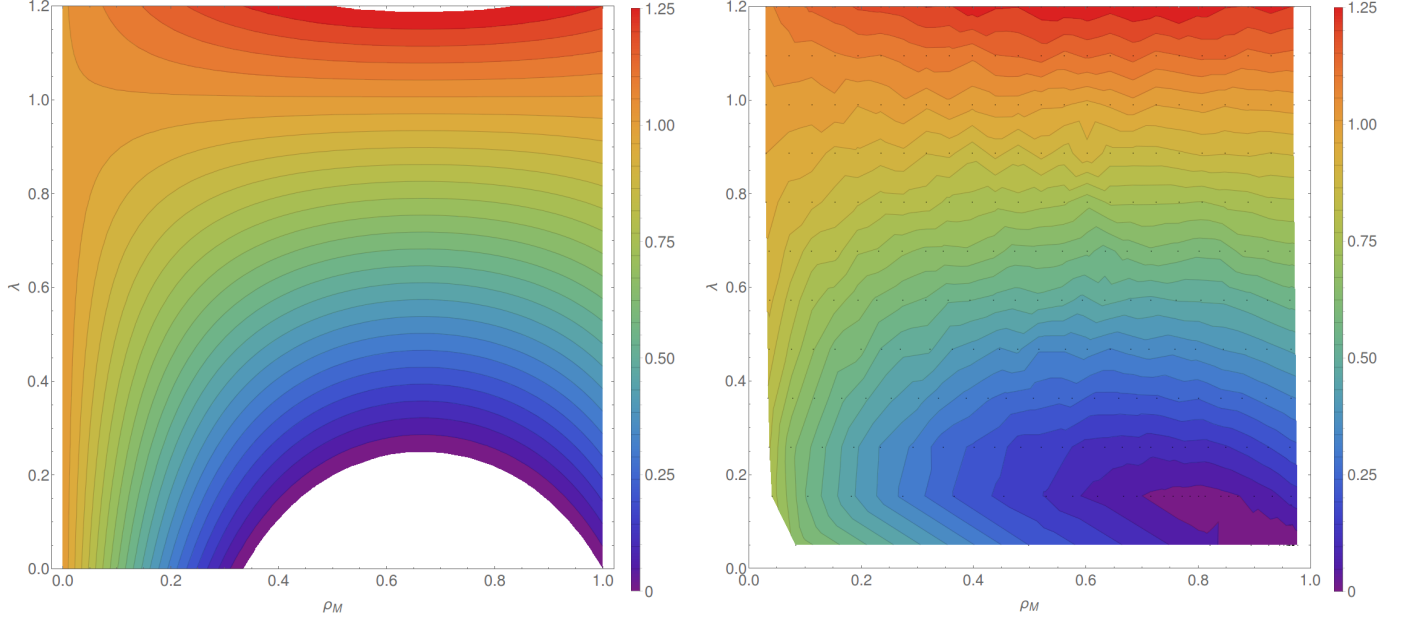
FIG. 3. The spacetime flow patterns, for the (λ, ρ_M) combinations indicated in the row and column headers. In each plot time runs along the x-axis, space along the y-axis. White represents full occupation, black empty, and grey shades partial occupation. The degree of occupation was calculated by taking the KMCLib record of a particular site's occupation (i.e. the Gillespie times at which the site changed occupation), assigning 0 and 1 to particles and vacancies respectively, linearly interpolating this and then integrating over times longer than a single Gillespie step but much shorter than the total time in question. In each case the total time elapsed is that taken by 10^6 Gillespie steps, and each short-time-average has been done over the total time divided by 508 (to produce square diagrams, as there are 508 active sites per simulation). Time has been rescaled this way in order to allow fair comparison of radically different λ-values.